Acta Mechanica 173, 207–222 (2004)
DOI 10.1007/s00707-004-0923-2

Acta Mechanica
Printed in Austria

Nonlinear microstructural constitutive equation of nanocrystalline metals

B. Wang, Harbin, China, and **Z. M. Xiao,** Singapore

Received April 24, 2001; revised October 12, 2001

Summary. Based on experimental observations, nanocrystalline materials are modeled as composite systems in which the amorphous interfacial phase is treated as the matrix, whereas the nano-scale single crystals are modeled as inclusions. Generally speaking, the elastic moduli of nanoscale crystals are higher than those of the amorphous matrix phase, and the deformation mechanism of nanocrystalline materials depends heavily on the size of the crystals. For conventional macro size crystal materials, such as coarse-grained polycrystalline materials, the deformation mechanism due to dislocation movement is dominant. When the crystal size is reduced to a certain critical value, plastic deformation is caused by shear banding in the amorphous matrix. In order to model such a deformation mechanism in nanocrystalline materials, constitutive equations are established based on internal variable theory. The proposed model reveals the relation between the yield strength and the grain size of the material.

1 Introduction

Nanostructured materials have a microstructure whose characteristic length scale is on the order of a few nanometers. Those materials consist of nanometer-sized crystallites with different crystallographic orientations and/or chemical compositions. The properties of nanocrystalline materials deviate from those of single crystals or coarse-grained polycrystals. This deviation results from the reduced size of the crystallites as well as from the numerous interfaces between adjacent crystallites. Nanostructured materials have been the subject of intensive study in the last decade [1]. Significant progress has been made in their processing and in the understanding of their fundamental properties. In this investigation, we focus our attention on developing a three-dimensional nonlinear constitutive equation for the deformation of nanocrystalline metals. On the one hand, the microstructural constitutive equation can provide a quantitative relation between material response and microstructural parameters, such as grain size. On the other hand, it can be adapted into a FEM code when one needs to carry out analysis on structures involving nanocrystalline materials.

Nanocrystalline materials have grain-size dependent mechanical properties which are significantly different to those of their coarser-grained counterparts. For example, nanophase metals are much stronger and apparently less ductile than conventional metals. Also nanophase ceramics are more ductile and more easily formed than conventional ceramics [2]. In addition, other structural features, such as pores, grain boundary junctions, and other crystal lattice defects that depend upon the fabrication and processing procedures, also play a significant role in the mechanical behavior of the materials. Therefore all the aforesaid structural aspects of nanophase materials must be considered in order to fully understand the mechanical behavior of these new materials. Extensive experimental observations have shown that nanocrystalline materials can be considered as composite systems consisting of essentially equiaxed grains and amorphous interfacial phase [3]. Owing to their ultrafine grain size, nanophase materials have a significant fraction of their atoms in grain boundaries. For an average grain diameter ranging between 5 and 10 nm, the percentage of the atoms in the interfacial phase can reach up to 50%, consequently the interfaces play a significant role in affecting the mechanical properties of nanophase materials. The boundary phase can be treated as an amorphous material and shows a lower elastic modulus and higher yield strength than the crystalline phase. It is well-known that the dominant plastic deformation mechanism for conventional coarse-grained metal is dislocation motion. For some nanocrystalline metals with a relatively large grain size, a dislocation-dominated plastic deformation mechanism was demonstrated by both atomic-scale computer simulations [4] and experimental observations [5]. When the grain sizes become smaller, the dislocation pile-ups cannot be supported [6]. In such a case, the dominant plastic deformation mechanism is due to the shear band formation in the amorphous phase. Experimental observations confirm that shear banding occurs in nanopolycrystalline materials [7], [8]. In addition to dislocation movement and shear banding, diffusional creep is a very important deformation process. Experimental observations reveal the enhanced atomic diffusion in nanocrystalline materials [9]. In this paper, we will not incorporate the diffusional creep deformation into our consideration. Interested readers are referred to the recent paper by Kim et al. [3].

In the current investigation, nanocrystalline materials are modeled as composites with nanoscale single crystals serving as the inclusion phase, while the amorphous interfacial phase is treated as the surrounding matrix phase. The matrix has a lower elastic modulus than that of the inclusions. Based on the deformation mechanism and the internal variable constitutive theory, in our study, the relation between the yield stress and grain sizes is predicted. It is found that for large grain materials the classical Hall-Petch relation is valid. For small grain materials, the yield stress is predicted to be constant if the elastic moduli of the crystalline phase and the amorphous phase are assumed to be the same, or it decreases with decreasing grain size if the elastic moduli of the two phases are different. Furthermore, a general form of incremental stress-strain relation is derived according to the deformation mechanism. The theory reveals the kinematic hardening behavior of nanocrystalline metals.

2 Microstructural characteristics and deformation mechanism of nanocrystalline materials

Many experimental techniques, such as TEM, HERM and X-ray analysis have provided evidence for the presence of “spread” grain boundary structures in nanocrystalline materials [10]. The intercrystalline volume fraction increases from about 0.3% at grain sizes ≥ 100 nm to greater than 50% at grain sizes of less than 5 nm. TEM has shown that many nanocrystalline materials are essentially equiaxed. If we further assume the grain is spherical with a uniform diameter d, and the grain boundary thickness is a constant δ, the total inter-crystalline volume fraction is approximately given by

$$v_m = 1 - \left(\frac{d-\delta}{d}\right)^3. \tag{1}$$

Figure 1 shows the calculated volume fraction v_f of the crystallite phase ($v_f = 1 - v_m$) as a function of the grain size by applying a boundary thickness of 1 nm [11], [12]. The total

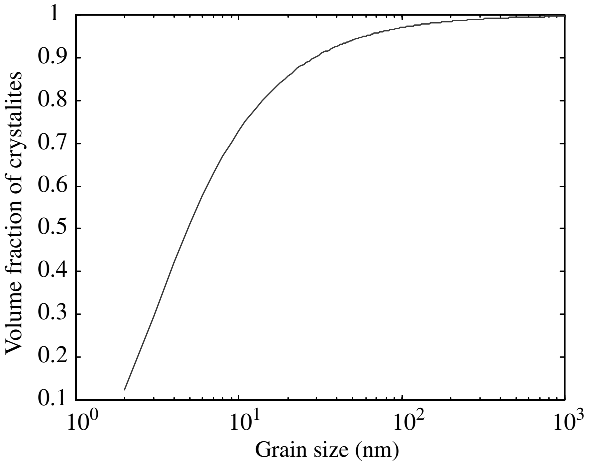

Fig. 1. The volume fraction of crystallites as a function of grain size

intercrystalline component is shown to be consistent with previous suggestions [13]. The interfacial region is believed to be composed of amorphous material. In general, the elastic modulus of the amorphous phase E_{am} is approximately 60–75% of that of the corresponding equilibrium crystalline alloy. There are evidences showing that the elastic modulus reduction of nanocrystalline material is due to the existence of the voids [8]. As we mentioned above, if the diffusion creep in nanocrystalline materials is neglected, there are two main deformation mechanisms dominating the plastic process. For those nanocrystalline materials with comparatively large grains, say, the grain size is larger than a few tens of nanometer, dislocations are generated at grain boundary ledges, and the material deforms plastically due to the dislocation pile-ups and movement. Since for such materials the grains are still much smaller than those in the conventional polycrystalline materials, the complex grain boundary structures will dominate the dislocation generation and movement. For those nanocrystalline materials with smaller grains, the dislocation activity is usually suppressed. The main plastic deformation mechanism is the shear band formation in the amorphous interfacial phase. Phenomenologically the stress-strain relation for amorphous materials approaches ideal plastic behavior. And in such case, the crystallites, playing the role of strengthening inclusion, will restrict the formation of the shear bands. In what follows, the general constitutive equation is derived by considering the two deformation mechanisms.

3 Internal variable constitutive theory

In a nonlinear deformation process, the thermodynamic state of a material element at a given time is not only a function of the instantaneous value of the strain ε_{ij}, but also depends upon the previous history of ε_{ij}. The investigation on the thermodynamic state can be dealt with in various manners. One effective method is "internal variable theory" [14], [15]. To completely define a thermodynamic state of a material, one needs to introduce some internal variables that describe the microstructural change of the material during loading, besides identifying the instantaneous strain. In such way, the dependence of the material response on loading history can be replaced by the dependence on what it has produced. Namely, the current pattern of structural arrangement on the microscale of the material element is represented by the current values of internal variables. When the internal variables are fixed, the response of the material depends only on the instantaneous value of the strain. However, the values of the internal variables depend on the loading history. The internal variable theory is based on the fundamental principle of thermodynamics. In its framework, one cannot only establish the relation between the stress and strain, but also derive the evolution equation of the microstructures based on the energy equilibrium concept. Consider a unit volume element of the material, its state variables are denoted as the strain tensor ε_{ij}, absolute temperature T and a group of internal variables ϑ_{ij}. In other words, the variables ε_{ij}, ϑ_{ij} and T can give a complete description for the state of the system. The first fundamental law of thermodynamics can be expressed in the following form:

$$dW = dU - dQ, \tag{2}$$

where U is the internal energy of the system, dW is the elementary work done on the system and dQ is the heat supply to the system.

The second fundamental law of thermodynamics states that there exists a state function $S(\eta_{ij}, \vartheta_k, T)$, called entropy, such that

$$TdS \geq dQ. \tag{3}$$

If (3) holds with the equality sign, the process is reversible, otherwise it is irreversible. The entropy can be written in the following form:

$$dS = d^{(r)}S + d^{(i)}S\ , \tag{4}$$

where

$$d^{(r)}S = \frac{dQ}{T} \tag{5}$$

is the reversible increment of S, called the entropy supply from outside, whereas

$$d^{(i)}S \geq 0 \tag{6}$$

is the irreversible increment, referred to the entropy production inside the system. The combination of (2), (3) and (4) leads to

$$dW = dU - dQ = dU - Td^{(r)}S = dU - TdS + Td^{(i)}S\ . \tag{7}$$

If the applied stress field on the material element is denoted as σ_{ij}, the elementary work done on the system can be written as

$$dW = \sigma_{ij} d\varepsilon_{ij}. \tag{8}$$

On account of the fact that U and S are state functions, Eq. (8) can be replaced by the relation

$$\sigma_{ij} d\varepsilon_{ij} = (\frac{\partial U}{\partial \varepsilon_{ij}} - T\frac{\partial S}{\partial \varepsilon_{ij}})d\varepsilon_{ij} + (\frac{\partial U}{\partial \vartheta_{ij}} - T\frac{\partial S}{\partial \vartheta_{ij}})d\vartheta_{ij} + (\frac{\partial U}{\partial T} - T\frac{\partial S}{\partial T})dT + Td^{(i)}S\ . \tag{9}$$

For the pure heating case, (9) is reduced to

$$\left(\frac{\partial U}{\partial T} - T\frac{\partial S}{\partial T}\right)dT + Td^{(i)}S = 0\ . \tag{10}$$

The second term in (10) is nonnegative according to (6). At the same time the quantity inside the parentheses of (10) is a state function and hence is independent of dT. Since (10) must hold for both positive and negative values of dT, we have

$$\frac{\partial U}{\partial T} - T\frac{\partial S}{\partial T} = 0\ . \tag{11}$$

It is noted that the above result is generally valid and independent of the choice of process even though we have obtained it by considering a special process. Equation (9) can be simplified if we introduce another state function, the free energy of the system defined by

$$\Xi = U - TS \, . \tag{12}$$

Then Eq. (9) is rewritten as

$$\sigma_{ij} d\varepsilon_{ij} = \frac{\partial \Xi}{\partial \varepsilon_{ij}} d\varepsilon_{ij} + \frac{\partial \Xi}{\partial \vartheta_{ij}} d\vartheta_{ij} + Td^{(i)}S. \tag{13}$$

As mentioned by Ziegler [15], the term $Td^{(i)}S$ has the form of elementary work, and can be expressed in the following form:

$$Td^{(i)}S = A_{ij} d\varepsilon_{ij} + B_{ij} d\vartheta_{ij} \, . \tag{14}$$

Substitution of Eq. (14) into Eq. (13) gives

$$\sigma_{ij} d\varepsilon_{ij} = \left(\frac{\partial \Xi}{\partial \varepsilon_{ij}} + A_{ij} \right) d\varepsilon_{ij} + \left(\frac{\partial \Xi}{\partial \vartheta_{ij}} + B_{ij} \right) d\vartheta_{ij} \, . \tag{15}$$

Since ε_{ij}, ϑ_{ij} are independent state variables, the above equation implies

$$\sigma_{ij} = \frac{\partial \Xi}{\partial \varepsilon_{ij}} + A_{ij} \, , \tag{16}$$

$$\frac{\partial \Xi}{\partial \vartheta_{ij}} + B_{ij} = 0 \, . \tag{17}$$

In fact, Eq. (16) is the constitutive relation of the material, and Eq. (17) can be used to determine the values of the internal variables.

We now rewrite Eq. (14) by replacing the differentials by time derivatives as follows:

$$\Phi = A_{ij} \dot{\varepsilon}_{ij} + B_{ij} \dot{\vartheta}_{ij} \, , \tag{18}$$

where Φ is the dissipation function which is the rate of work done by the dissipation forces. Equation (18) cannot determine the dissipation force, neither the tensors A_{ij} and B_{ij}, even if the dissipation function is obtained. Instead, Eq. (18) determines their magnitude once the direction, i.e., the ratio of the components, is known. To determine the tensors A_{ij} and B_{ij}, we introduce the following orthogonality condition: the dissipation force corresponding to the velocity $\dot{\varepsilon}_{ij}$ or $\dot{\vartheta}_{ij}$ is orthogonal to the dissipation surface $\Phi = \Phi_0$ at the end point. Therefore we obtain

$$\begin{aligned} A_{ij} &= \lambda_1 \frac{\partial \Phi}{\partial \dot{\varepsilon}_{ij}} \, , \\ B_{ij} &= \lambda_2 \frac{\partial \Phi}{\partial \dot{\vartheta}_{ij}} \, , \end{aligned} \tag{19}$$

where λ_1, λ_2 are proportional factors determined with the aid of (18), given by

$$\begin{aligned} \lambda_1 &= \left(\frac{\partial \Phi}{\partial \dot{\varepsilon}_{ij}} \dot{\varepsilon}_{ij} \right)^{-1} \Phi \, , \\ \lambda_2 &= \left(\frac{\partial \Phi}{\partial \dot{\vartheta}_{ij}} \dot{\vartheta}_{ij} \right)^{-1} \Phi \, . \end{aligned} \tag{20}$$

It is worth to note that as discussed by Ziegler [15], the orthogonality condition is equivalent to the principle of maximal dissipation rate.

4 Dislocation-dominated deformation mechanism for nanocrystalline materials with comparatively large grain size

In this part, we will establish the constitutive equation of the nanocrystalline materials governed by the deformation mechanism of intragrain dislocation movement. The material can be treated as a composite system whose inclusions have plastic deformation due to dislocation motion, and whose amorphous matrix deforms elastically only with a lower elastic modulus than that of the inclusions. The deformation of the crystallite is assumed to follow the elastic and non-hardening plastic Mises yielding criterion. By considering the hardening effect of the grain boundary, the yield stress is expressed as a decreasing function of grain size according to the Hall-Petch relation as

$$f_1(\sigma_{ij}^c) = \sqrt{J_2} - (\sigma_y + \frac{k_y}{\sqrt{d}}) = 0\ , \tag{21}$$

where d is the grain diameter, and σ_y, k_y are temperature-dependent material constants. $J_2(=\frac{1}{2}s_{ij}s_{ij})$ is the second principle invariant of the stress deviator with

$$s_{ij} = \sigma_{ij} - \sigma_m \delta_{ij}. \tag{22}$$

Consider a unit volume of a nanocrystalline material, in which the spherical crystallites with the plastic strain ε_{ij}^p are distributed in the amorphous matrix. In this part the plastic strains are denoted as the internal variables. If ε_{ij}^0 is denoted as the strain field created by the applied traction in the absence of the plastic strain, according to Colonnetti's theorem [16], the strain energy for the case when ε_{ij}^0 and ε_{ij}^p coexist is the sum of those elastic energies for the cases when the applied load and the plastic strain exist alone, respectively. Therefore, if the element is subjected to an applied surface traction without any plastic deformation, the elastic strain energy becomes

$$\Xi_1 = \frac{1}{2}\int_D (\sigma_{ij}^0 + \sigma_{ij}^{'})(\varepsilon_{ij}^0 + \varepsilon_{ij}^{'})dv, \tag{23}$$

where ε_{ij}^0 is the applied external strain, σ_{ij}^0 is the corresponding stress field if the inclusions have the same elastic modulus as the matrix; $\sigma_{ij}^{'}$, $\varepsilon_{ij}^{'}$ are the perturbations of stress and strain fields induced by the existences of the crystallites. Use $u_i^{'}$ denoting the perturbation of the displacement field, on the boundary of the element,

$$u_i^{'} = 0\ , \quad \text{on} \quad S. \tag{24}$$

Therefore,

$$\int_D (\sigma_{ij}^0 + \sigma_{ij}')\varepsilon_{ij}'dv = \iint_S (\sigma_{ij}^0 + \sigma_{ij}')n_j u_i' dv - \int_D (\sigma_{ij}^0 + \sigma_{ij}')_{,j} u_i' dv = 0,$$

$$\int_D \sigma_{ij}'\varepsilon_{ij}^0 dv = \int_D C_{ijkl}(\varepsilon_{kl}' - \varepsilon_{kl}^*)\varepsilon_{ij}^0 dv = -\int_D \sigma_{ij}^0 \varepsilon_{ij}^* dv, \tag{25}$$

where ε_{ij}^* is the fictitious eigenstrain introduced in the equivalent inclusion method [16]. Substitution of Eq. (25) into Eq. (23) yields

$$\Xi_1 = \frac{1}{2}\int_D \sigma_{ij}^0 \varepsilon_{ij}^0 dv - \frac{1}{2}\int_D \sigma_{ij}^0 \varepsilon_{ij}^* dv = \frac{1}{2}(\sigma_{ij}^0 \varepsilon_{ij}^0 - v_f \sigma_{ij}^0 \varepsilon_{ij}^*), \tag{26}$$

where v_f is the volume fraction of the crystallite phase. One can notice that the sign of the last term in Eq. (26) is different from Mura's result. This is because we assume that the given term is the strain field ε_{ij}^0 instead of the stress field σ_{ij}^0. The fictitious eigenstrain ε_{ij}^* can be determined by using the Mori and Tanaka method [17] to consider the interaction among the inclusions, which is shown in Appendix 1 in detail. For isotropic, spherical crystallites, one can express the energy in the form of

$$\Xi_1 = \frac{1}{2}(2\bar{\mu}E^1_{ijkl} + \bar{\lambda}E^2_{ijkl})\varepsilon^0_{ij}\varepsilon^0_{kl} , \tag{27}$$

where

$$\begin{aligned}
&E^1_{ijkl} = \frac{1}{2}(\delta_{ik}\delta_{jl} + \delta_{il}\delta_{jk}), \quad E^2_{ijkl} = \delta_{ij}\delta_{kl} , \\
&\quad \bar{\mu} = \mu - v_f\mu\Gamma_1 , \\
&\quad \bar{\lambda} = \lambda - v_f(\lambda\Gamma_1 + 2\mu\Gamma_2 + 3\lambda\Gamma_2) , \\
&\quad \Gamma_1 = 2(\mu^* - \mu)/\omega_1 , \\
&\quad \Gamma_2 = (\lambda^* - \lambda)/\omega_1 - 2\omega_2(\mu^* - \mu)/[\omega_1(\omega_1 + 3\omega_2)] - 3(\lambda^* - \lambda)\omega_2/[\omega_1(\omega_1 + 3\omega_2)] , \\
&\quad \omega_1 = 2(1 - v_f)(\mu - \mu^*)S_1 - 2\mu , \\
&\quad \omega_2 = 2(1 - v_f)(\mu - \mu^*)S_2 + (1 - v_f)S_1(\lambda - \lambda^*) + 3(1 - v_f)(\lambda - \lambda^*)S_2 - \lambda , \\
&\quad S_1 = 2(4 - 5\gamma)/[15(1 - \gamma)], \quad S_2 = (5\gamma - 1)/[15(1 - \gamma)] ,
\end{aligned} \tag{28}$$

in which $\mu,\ \lambda,\ \mu^*, \lambda^*$ are Lamé constants of the amorphous matrix and crystallites, respectively, γ is and Poisson's ratio of the matrix. As mentioned above, under isothermal conditions, the state variables are the total strain tensor ε_{ij} and the internal variables ε^p_{ij} for our system. Therefore we need to express the elastic energy as a function of the total strain and the plastic strain. The total strain of the material element can be expressed in the form of

$$\varepsilon_{ij} = \varepsilon^0_{ij} + \varepsilon^D_{ij}, \tag{29}$$

where ε^0_{ij} is the applied elastic strain without any plastic deformation, ε^D_{ij} is the volume average strain created by the plastic deformation inside the crystallites. If the crystallites have the same elastic modulus as the matrix, $\varepsilon^D_{ij} = v_f\varepsilon^p_{ij}$. Since the elastic modulus of the crystallite phase is different from that of the amorphous matrix, we can adapt the Mori-Tanaka method to determine the volume average of the plastic strain as (Appendix 2)

$$\varepsilon^D_{ij} = v_f D_{ijkl}\varepsilon^p_{kl} , \tag{30}$$

where

$$\begin{aligned}
&D_{ijkl} = D_1E^1_{ijkl} + D_2E^2_{ijkl} , \\
&\quad D_1 = 2\mu^*/B_1 , \\
&\quad D_2 = \lambda^*/B_1 - 2\mu^*B_2/[B_1(B_1 + 3B_2)] - 3\lambda^*B_2/[B_1(B_1 + 3B_2)] , \\
&\quad B_1 = 2[\mu^* + (1 - v_f)(\mu^* - \mu)(S_1 - 1)] , \\
&\quad B_2 = \lambda^* + (1 - v_f)[2S_2(\mu^* - \mu) + (S_1 - 1)(\lambda^* - \lambda) + 3S_2(\lambda^* - \lambda)] ,
\end{aligned} \tag{31}$$

in which all the symbols are the same as in Eq. (28).

Now we consider the other part of the elastic energy produced by the plastic deformation in the crystallites:

$$\Xi_2 = \frac{1}{2}\int_D \sigma_{ij}(\varepsilon_{ij} - \varepsilon^p_{ij}H[\Sigma\Omega_k])dv , \tag{32}$$

with

$$H[\Sigma\Omega_k] = \begin{cases} 1 & x \in \Sigma\Omega_k \ , \\ 0 & x \notin \Sigma\Omega_k , \end{cases} \tag{33}$$

where $\Sigma\Omega_k$ is the region occupied by the crystallite phase. Since the traction on the boundary of the element is absent, we have

$$\int\limits_d \sigma_{ij}\varepsilon_{ij} dv = \iint\limits_S \sigma_{ij} n_j u_i ds - \int\limits_D \sigma_{ij,j} u_i dv = 0 \ . \tag{34}$$

Equation (32) is thus rewritten as

$$\Xi_2 = -\frac{1}{2}\Sigma \int\limits_{\Omega_k} \sigma_{ij}\varepsilon_{ij}^p dv = -\frac{1}{2} v_f \sigma_{ij}\varepsilon_{ij}^p \ , \tag{35}$$

where σ_{ij} is the stress field in the crystallite induced by the plastic deformation. By using Mori-Tanaka average field method, the stress field inside the crystallite is derived as (Appendix 2)

$$\sigma_{ij} = G_{ijkl}\varepsilon_{kl}^p \ , \tag{36}$$

where

$$\begin{aligned} G_{ijkl} &= G_1 E_{ijkl}^1 + G_2 E_{ijkl}^2 , \\ G_1 &= 2(1 - v_f)\mu(S_1 - 1)D_1 , \\ G_2 &= (1 - v_f)\{2D_2\mu(S_1 - 1) + D_1[2\mu S_2 + \lambda(S_1 - 1) + 3\lambda S_2] + 3D_2[2\mu S_2 + \lambda(S_1 - 1) + 3\lambda S_2]\} , \end{aligned} \tag{37}$$

in which all the symbols have the same meaning given in Eqs. (28) and (31). By taking the sum of Eqs. (27) and (35) and substituting the corresponding quantities, one can write the total elastic energy of the system as

$$\Xi = \Xi_1 + \Xi_2 = \frac{1}{2}(2\bar{\mu}E_{ijkl}^1 + \bar{\lambda}E_{ijkl}^2)(\varepsilon_{ij} - v_f D_{ijmn}\varepsilon_{mn}^p)(\varepsilon_{kl} - v_f D_{klmn}\varepsilon_{mn}^p) - \frac{1}{2} v_f G_{ijkl}\varepsilon_{ij}^p\varepsilon_{kl}^p \ . \tag{38}$$

Since the crystallites undergo the plastic deformation which induces energy dissipation, the energy dissipation rate in unit volume can be expressed in the form of

$$\Phi = v_f \sigma_{ij}^c \dot{\varepsilon}_{ij}^p \ , \tag{39}$$

where σ_{ij}^c is the resistance tensor of the plastic deformation and satisfies the yielding condition (21), and $\dot{\varepsilon}_{ij}^p$ is the rate of the plastic deformation. One should bear in mind that only under the loading condition beyond the yielding point the energy dissipation rate is not zero. Under the unloading condition or in the stage of elastic deformation, $\dot{\varepsilon}_{ij}^p = 0$.

Substituting the energy Eq. (38) into Eq. (16), and noticing $A_{ij} = 0$ for the dissipation potential given by Eq. (39), one can derive the constitutive equation as

$$\sigma_{ij} = (2\bar{\mu}E_{ijkl}^1 + \bar{\lambda}E_{ijkl}^2)(\varepsilon_{kl} - v_f D_{klmn}\varepsilon_{mn}^p) \ , \tag{40}$$

or in rate form as

$$\dot{\sigma}_{ij} = \bar{C}_{ijkl}(\dot{\varepsilon}_{kl} - v_f D_{klmn}\dot{\varepsilon}_{mn}^p) = (2\bar{\mu}E_{ijkl}^1 + \bar{\lambda}E_{ijkl}^2)(\dot{\varepsilon}_{kl} - v_f D_{klmn}\dot{\varepsilon}_{mn}^p) \ . \tag{41}$$

The change rate of plastic deformation can be determined through the evolution Eq. (17) as

$$\sigma_{ij}^c = D_{ijmn}\sigma_{mn} + G_{ijmn}\varepsilon_{mn}^p \ , \tag{42}$$

where σ_{mn} is the applied stress determined by Eq. (40). Substitution of Eq. (42) into the yielding condition of the crystallite, Eq. (21), gives the loading surface of the composite material. As expected, it is seen that the material behaves as a kinematic hardening material [18]. If $\varepsilon_{ij}^p = 0$, combination of Eqs. (21) and (42) gives the initial yield surface of the material. Using the loading surface, the criterion for loading can be written in the form

$$f_1(\sigma_{ij}^c) = 0, \quad \frac{\partial f_1}{\partial \sigma_{ij}} \cdot \dot{\sigma}_{ij} > 0 \; . \tag{43}$$

Further by substituting Eq. (40) into Eq. (42), then into Eq. (21), and taking the derivative with respect to time, one can obtain

$$\frac{\partial f_1}{\partial \sigma_{ij}^c} \{ D_{ijkl} \bar{C}_{klmn} \dot{\varepsilon}_{mn} + [G_{ijmn} - v_f D_{ijkl} \bar{C}_{kl\alpha\beta} D_{\alpha\beta mn}] \dot{\varepsilon}_{mn}^p \} = 0 \; . \tag{44}$$

By using the Prandtl-Reuss [19] material model, the rate of the plastic deformation can be written as

$$\dot{\varepsilon}_{mn}^p = \dot{\lambda} \frac{\partial f_1}{\partial \sigma_{mn}^c} \; . \tag{45}$$

Substituting Eq. (45) into Eq. (44) and solving for $\dot{\lambda}$, we have

$$\dot{\lambda} = \frac{\partial f_1 / \partial \sigma_{ij}^c D_{ijkl} \bar{C}_{klmn}}{\partial f_1 / \partial \sigma_{ij}^c [v_f D_{ijkl} \bar{C}_{kl\alpha\beta} D_{\alpha\beta mn} - G_{ijmn}] \partial f_1 / \partial \sigma_{mn}^c} \dot{\varepsilon}_{mn} = \Delta_{mn} \dot{\varepsilon}_{mn} \; . \tag{46}$$

Substituting Eq. (46) into Eq. (45), then into Eq. (41), one obtains the incremental stress-strain relation as

$$\dot{\sigma}_{ij} = C_{ijkl}^P \dot{\varepsilon}_{kl} = \bar{C}_{ijmn} \left(E_{mnkl}^1 - \frac{v_f D_{mn\alpha\beta} b \partial f_1}{\partial \sigma_{\alpha\beta}^c \Delta_{kl}} \right) \dot{\varepsilon}_{kl} \; . \tag{47}$$

It is worth to note that the incremental stress-strain relation given in Eq. (47) is the most convenient form for it to be implemented into a FEM code.

5 Deformation mechanism by shear banding in amorphous interfacial phases for nanocrystalline materials with smallsize grain

The amorphous interfacial phase in nanocrystalline metals behaves as metallic glasses. In fact, the typical deformation mechanism for metal glasses is shear band formation. Due to this deformation mechanism, the tension behavior of the materials is quite different to the compression behavior although they can be described as elastic-perfectly plastic materials. Research activities related to metallic glasses have been greatly enhanced recently. Donovan [20] studied plastic deformation of a Pd-Ni-P glass and concluded that the onset of yielding was best described by the Mohr-Coulomb law in which the normal stress on a particular plane affects the critical shear stress at which yielding begins to occur. According to this law, the shear stress τ for yielding is given by

$$f_2 = \tau - (\tau_y - \alpha \sigma_n) = 0, \tag{48}$$

where τ_y is the yield stress in pure shear and σ_n is the normal tensile stress acting on the active slip plane, α is another material constant.

In this paper, we assume that the amorphous interfacial phase can be described as elastic-perfectly plastic material, and the yielding is described by the Mohr-Coulomb law given in Eq. (48). In such case, the crystallite phase deforms elastically. Therefore we will restrict plastic deformation to that of the amorphous matrix, as the strengthening second phase in dispersion hardening alloys. Under a given loading history, for simplicity, the plastic deformation ε_{ij}^{pm} in the uniform amorphous matrix without any elastic crystallite phase is assumed to be uniform. Since uniform plastic strain over the entire body does not produce internal stress, the internal stress and the elastic energy induced by the prescribed plastic deformation in the matrix are calculated by considering the situation, where

$\varepsilon_{ij}^{p} = 0$ in the matrix,

$\varepsilon_{ij}^{p} = -\varepsilon_{ij}^{pm}$ in the crystallites.

The elastic energy given by Eqs. (27) and (35) is still the same, but the overall plastic strain becomes

$$\varepsilon_{ij}^{D} = \varepsilon_{ij}^{pm} - v_f D_{ijkl}\varepsilon_{kl}^{pm} = (E_{ijkl}^{1} - v_f D_{ijkl})\varepsilon_{kl}^{pm} \ . \tag{49}$$

Substituting Eq. (49) into Eq. (29), then into Eq. (27) and (35), one obtains the total elastic energy

$$\begin{aligned}\Xi = \Xi_1 + \Xi_2 = \frac{1}{2}(2\bar{\mu}E_{ijkl}^{1} + \bar{\lambda}E_{ijkl}^{2})[\varepsilon_{ij} - (E_{ijmn} - v_f D_{ijmn})\varepsilon_{mn}^{pm}][\varepsilon_{kl} - (E_{klmn}^{1} - v_f D_{klmn})\varepsilon_{mn}^{pm}] \\ - \frac{1}{2}v_f G_{ijkl}\varepsilon_{ij}^{pm}\varepsilon_{kl}^{pm} \ .\end{aligned} \tag{50}$$

The energy dissipation rate in unit volume can be expressed in the form

$$\Phi = (1 - v_f)\sigma_{ij}^{cm}\dot{\varepsilon}_{ij}^{pm} \ , \tag{51}$$

where σ_{ij}^{cm} is the resistance force of the plastic deformation and satisfies the yielding condition (48). In the same manner as deriving Eq. (41), we can derive the stress-strain rate relation as

$$\begin{aligned}\dot{\sigma}_{ij} &= \bar{C}_{ijkl}[\dot{\varepsilon}_{kl} - (E_{klmn}^{1} - v_f D_{klmn})\dot{\varepsilon}_{mn}^{pm}] \\ &= (2\bar{\mu}E_{ijkl}^{1} + \bar{\lambda}E_{ijkl}^{2})[\dot{\varepsilon}_{kl} - (E_{klmn}^{1} - v_f D_{klmn})\dot{\varepsilon}_{mn}^{pm}] \ .\end{aligned} \tag{52}$$

The change rate of the plastic deformation can be determined through the evolution Eq. (17) as

$$\sigma_{ij}^{cm} = [(E_{ijmn}^{1} - v_f D_{ijmn})\sigma_{mn} + v_f G_{ijmn}\varepsilon_{mn}^{p}]/(1 - v_f) \ . \tag{53}$$

Substitution of Eq. (53) into the yielding condition of the crystallite, Eq. (48), gives the loading surface of the composite material. It can be seen that the material also behaves as a kinematic hardening material.

In the same way as deriving Eq. (47), one can obtain the final stress-strain rate relation under the loading condition as

$$\dot{\sigma}_{ij} = C_{ijkl}^{P}\dot{\varepsilon}_{kl} = \bar{C}_{ijmn}[E_{mnkl}^{1} - \frac{(E_{mn\alpha\beta}^{1} - v_f D_{mn\alpha\beta})\partial f_2}{\partial\sigma_{\alpha\beta}^{cm}\Delta_{kl}^{m}}]\dot{\varepsilon}_{kl} \ , \tag{54}$$

with

$$\Delta_{mn}^{m} = \frac{\partial f_2/\partial\sigma_{ij}^{cm}(E_{ijkl}^{1} - v_f D_{ijkl})\bar{C}_{klmn}}{\partial f_2/\partial\sigma_{ij}^{cm}[(E_{ijkl}^{1} - v_f D_{ijkl})\bar{C}_{kl\alpha\beta}(E_{\alpha\beta mn}^{1} - v_f D_{\alpha\beta mn}) - v_f G_{ijmn}]\partial f_2/\partial\sigma_{mn}^{cm}} \ . \tag{55}$$

6 Comparison between the theoretical prediction and experiments

6.1 *Effective elastic modulus*

It is generally believed that the elastic moduli of nanocrystalline materials are lower than those of their coarse-grain counterparts due to the low density of the amorphous interfacial phase. Recently, nanocrystalline materials were fabricated by controlled annealing of amorphous

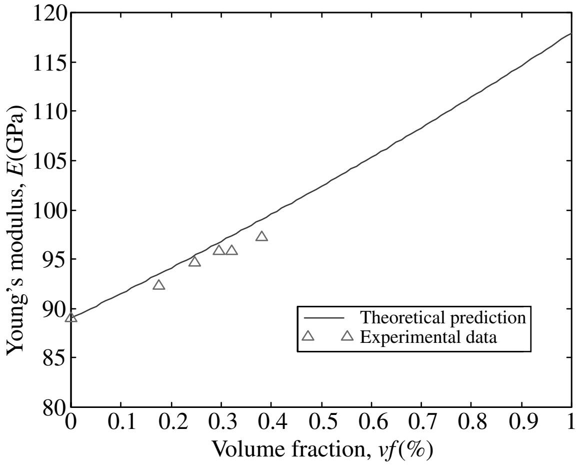

Fig. 2. The effective Young's modulus of bulk $Zr_{53}Ti_5Ni_{10}Cu_{20}Al_{12}$ alloy versus the volume fraction of crystallites

alloys between the glass transition temperature and the crystallization temperature [21], [22]. In the current study, we use the data of bulk $Zr_{53}Ti_5Ni_{10}Cu_{20}Al_{12}$ alloy obtained by Fan et al. [21] to verify our elastic modulus prediction. The elastic constants of the amorphous matrix and nanoparticles can be taken as

$$\mu = 34.23 \text{ GPa}, \quad \lambda = 51.35 \text{ GPa}, \quad \mu^* = 45.5 \text{ GPa}, \ \lambda^* = 66 \text{ GPa},$$

respectively. The elastic moduli tensor obtained by this model is given by

$$\bar{C}_{ijkl} = 2\bar{\mu}E^1_{ijkl} + \bar{\lambda}E^2_{ijkl}, \tag{56}$$

where the effective Lamé constants $\bar{\lambda}$, $\bar{\mu}$ of the nanocrystalline material are given by Eq. (28) explicitly. After determining $\bar{\lambda}$, $\bar{\mu}$, one can obtain the effective Young's modulus for the composite system. The Young's modulus versus the volume fraction of the nanoparticles is plotted in Fig. 2. Since the elastic mismatch between the two phase materials is small, the effective modulus of the composite system almost increases linearly with the volume fraction of the inclusions as shown in Fig. 2, in which the experimental data of Fan et al. [21] for Young's modulus were also given.

6.2 Dependence of yield stress on the grain size

The relation between yield stress and grain size has been the subject of intensive research in recent years due to the complex behavior observed in nanophase materials. Most of the results obtained confirm the validity of the classical Hall-Petch relation down to grain sizes of the order of a few tens of nanometers [8]. When the grain size is further reduced below this value, the results obtained are controversial. Many experimental results indicate a yield stress independent of the grain size, or even reverse H-P relation, i.e., the yield stress will decrease with decreasing grain size. According to the work of Sanders et al. [8], the reduction in elastic modulus is mainly due to the porosity of the samples of the nanocrystalline materials. For high density and high-purity nanocrystalline materials, only small decrements from coarse-grained values observed in the Young's modulus are caused primarily by the slight amount of porosity in the samples. In this part, we derive the relation between the yield stress and the grain size by assuming the two phases of the material have the same elastic modulus. For homogenous material, the stresses both inside the inclusion and in the matrix are uniform if plastic deformation has not occurred. When the size of the grain becomes smaller, the shear banding deformation mechanism dominates. The uniaxial yield stress is constant and determined by

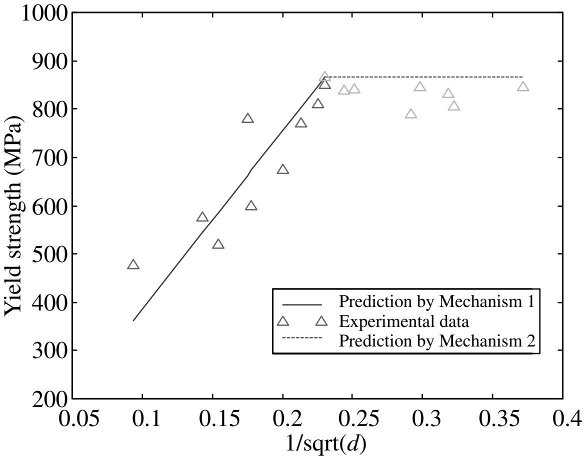

Fig. 3. The yield strength of nanocrystalline Cu versus the grain size $1/\sqrt{d}$ $(nm)^{-\frac{1}{2}}$

Eqs. (48) and (53). For materials exhibiting little work hardening, the ratio of the Vickers microhardness to the yield strength is ≈ 3 [23]. According to the hardness measurements on over 30 nanocrystalline Cu samples with a grain size ranging from < 10 nm to > 100 nm, the corresponding yield strength was in general agreement with the coaser-grained Hall-Petch relationship down to a grain size of ≈16 nm, at this point the yield strength leveled off and approached a constant value [30]. Based on the above two deformation models, the theory predicts exactly such a trend. The yield stress as a function of the grain size is shown in Fig. 3.

7 Conclusions

In this paper, based on the microstructural characteristics and the two deformation mechanisms, dislocation movement inside the crystallite and shear banding in the amorphous matrix of nanocrystalline metals, a general form of constitutive model for nanocrystalline materials was developed. The material was modeled as a composite system with one phase being able to undergo plastic deformation. An energy approach was adopted to derive the hardening rule and the incremental stress-strain relation of nanocrystalline materials. Recently, due to the pioneer works by Fleck and Hutchinson [25], Hutchinson [26], Gao et al. [27], Huang et al. [28], etc, the theory of strain gradient plasticity became a very active research direction. In the current study, we emphasize that only the microstructures of the material are in nanoscale, whereas the wavelength of the overall deformation is much larger than the size of the microstructures. Therefore we do not need to incorporate the formulation of strain gradient plasticity. The constitutive equations obtained can be easily implemented into a FEM code when there is a need for numerical simulation of nanocrystalline materials and structures.

Appendix 1

Determination of the fictitious eigenstrain ε_{ij}^{*}

Consider that in an elastic matrix there is a random distribution of inclusions. The elastic moduli tensors of the matrix and inclusions are C_{ijkl}, C_{ijkl}^{*}, respectively. The composite element is subjected to an external applied strain field ε_{ij}^{0}. Under such condition, we assume that the average strain field in the matrix is ε_{ij}^{M}. To incorporate the interaction effect of the inclusions, we further assume that every single inclusion is subjected to the strain field ε_{ij}^{M}, instead of ε_{ij}^{0}. According to the equivalent inclusion principle [16], [29], the stress field inside an inclusion can be expressed in the following form:

$$C^{*}_{ijkl}(\varepsilon^{M}_{kl}+\varepsilon'_{kl}) = C_{ijkl}(\varepsilon^{M}_{kl}+\varepsilon'_{kl}-\varepsilon^{*}_{kl}) \tag{A.1}$$

which defines the fictitious eigenstrain ε^{*}_{kl}, and ε'_{kl} is the perturbation of strain field due to the existence of the inclusion, and is given by

$$\varepsilon'_{kl} = S_{klmn}\varepsilon^{*}_{mn}, \tag{A.2}$$

where S_{klmn} is Eshelby's tensor.

Since the volume average of the strain field should be equal to the applied strain field, one can write

$$v_f(\varepsilon^{M}_{ij}+\varepsilon'_{ij}) + (1-v_f)\varepsilon^{M}_{ij} = \varepsilon^{o}_{ij}\ . \tag{A.3}$$

From the above three equations, one can derive

$$\varepsilon^{*}_{ij} = \Gamma_{ijkl}\varepsilon^{0}_{kl}\ , \tag{A.4}$$

where

$$\Gamma_{ijkl} = [\mathbf{C}+(1-v_f)(\mathbf{C}^{*}-\mathbf{C})\mathbf{S}]^{-1}_{ijmn}(C^{*}_{mnkl}-C_{mnkl})\ . \tag{A.5}$$

For isotropic material, we have

$$\begin{aligned} C^{*}_{ijkl} &= 2\mu^{*}E^{1}_{ijkl}+\lambda^{*}E^{2}_{ijkl}\ , \\ C_{ijkl} &= 2\mu E^{1}_{ijkl}+\lambda E^{2}_{ijkl}\ , \end{aligned} \tag{A.6}$$

where μ, λ, μ^{*}, λ^{*} are Lamé constants of the matrix and inclusions, respectively, and

$$E^{1}_{ijkl} = \frac{1}{2}(\delta_{ik}\delta_{jl}+\delta_{il}\delta_{jk}), \qquad E^{2}_{ijkl} = \delta_{ij}\delta_{kl}\ . \tag{A.7}$$

For spherical inclusion, Eshelby's tensor can be expressed in the form

$$S_{ijkl} = S_1E^{1}_{ijkl}+S_2E^{2}_{ijkl}\ , \tag{A.8}$$

where $S_1 = 2(4-5\gamma)/[15(1-\gamma)]$, $S_2 = (5\gamma-1)/[15(1-\gamma)]$, and γ is Poisson's ratio of the matrix. By introducing the tensors E^{1}_{ijkl}, E^{2}_{ijkl}, we can simplify our analysis. Since

$$\begin{aligned} &E^{1}_{ijkl}\cdot E^{1}_{klmn} = E^{1}_{ijmn}, \quad E^{1}_{ijkl}\cdot E^{2}_{klmn} = E^{2}_{ijmn}, \quad E^{2}_{ijkl}\cdot E^{2}_{klmn} = 3E^{2}_{ijmn}\ , \\ &(aE^{1}_{ijkl}+bE^{2}_{ijkl})\cdot\left\{\frac{1}{aE^{1}_{klmn}}-\frac{b}{[a(a+3b)]}E^{2}_{klmn}\right\} = E^{1}_{ijmn}\ , \end{aligned} \tag{A.9}$$

substituting Eqs. (A.6), (A.7) into Eq. (A.5), and using Eq. (A.9), we obtain

$$\varepsilon^{*}_{ij} = (\Gamma_1E^{1}_{ijkl}+\Gamma_2E^{2}_{ijkl})\varepsilon^{0}_{kl}\ , \tag{A.10}$$

where

$$\begin{aligned} \Gamma_1 &= 2(\mu^{*}-\mu)/\omega_1, \\ \Gamma_2 &= (\lambda^{*}-\lambda)/\omega_1 - 2\omega_2(\mu^{*}-\mu)/[\omega_1(\omega_1+3\omega_2)] - 3(\lambda^{*}-\lambda)\omega_2/[\omega_1(\omega_1+3\omega_2)]\ , \\ \omega_1 &= 2(1-v_f)(\mu-\mu^{*})S_1 - 2\mu\ , \\ \omega_2 &= 2(1-v_f)(\mu-\mu^{*})S_2 + (1-v_f)S_1(\lambda-\lambda^{*}) + 3(1-v_f)(\lambda-\lambda^{*})S_2 - \lambda\ . \end{aligned} \tag{A.11}$$

In essence, the assumption taken in this part is the same as Mori-Tanaka theory for random distribution of the inclusions.

Appendix 2

Determination of the overall strain and the stress inside an inclusion created by the plastic deformation

In the amorphous matrix, the problem now becomes that there is a random distribution of inclusions with a plastic strain ε^p_{ij}. The applied stress field on the material element is absent in this case. We need to derive the volume average strain and the stress field inside a single inclusion due to the plastic deformation. According to the equivalent inclusion principle, we have

$$C^*_{ijkl}(\varepsilon^M_{kl} + S_{klmn}\varepsilon^{**}_{mn} - \varepsilon^p_{kl}) = C_{ijkl}(\varepsilon^M_{kl} + S_{klmn}\varepsilon^{**}_{mn} - \varepsilon^{**}_{kl}) \ , \tag{A.12}$$

where $\varepsilon^{**}_{kl} = \varepsilon^p_{kl} + \varepsilon^*_{kl}$ is the total eigenstrain due to the plastic deformation and the elastic modulus mismatch. Since the applied stress is absent, the volume average of the stress field is zero, therefore

$$v_f C_{mnij}(\varepsilon^M_{ij} + S_{ijkl}\varepsilon^{**}_{kl} - \varepsilon^{**}_{ij}) + (1 - v_f)C_{mnij}\varepsilon^M_{ij} = 0. \tag{A.13}$$

From Eqs. (A.12) and (A.13), one can obtain the total eigenstrain ε^{**}_{kl} as

$$\begin{aligned} \varepsilon^{**}_{ij} &= [\mathbf{C} * + (1 - v_f)(\mathbf{C}^* - \mathbf{C})(\mathbf{S} - \mathbf{E}^1)]^{-1}_{ijkl} C^*_{klmn}\varepsilon^p_{mn} \ , \\ \varepsilon^M_{ij} &= -v_f(S_{ijkl} - E^1_{ijkl})\varepsilon^{**}_{kl} \ . \end{aligned} \tag{A.14}$$

The stress field inside a single inclusion can be obtained in the form

$$\sigma_{ij} = C_{ijkl}(\varepsilon^M_{kl} + S_{klmn}\varepsilon^{**}_{mn} - \varepsilon^{**}_{kl}) = G_{ijkl}\varepsilon^p_{kl} \ , \tag{A.15}$$

and for isotropic material and spherical inclusion

$$\begin{aligned} G_{ijkl} &= G_1 E^1_{ijkl} + G_2 E^2_{ijkl} \ , \\ G_1 &= 2(1 - v_f)\mu(S_1 - 1)D_1 \ , \\ G_2 &= (1 - v_f)\{2D_2\mu(S_1 - 1) + D_1[2\mu S_2 + \lambda(S_1 - 1) + 3\lambda S_2] \\ &\quad + 3D_2[2\mu S_2 + \lambda(S_1 - 1) + 3\lambda S_2]\} \ , \end{aligned}$$

with

$$\begin{aligned} D_1 7 &= 2\mu^*/B_1 \ , \\ D_2 &= \lambda^*/B_1 - 2\mu^* B_2/[B_1(B_1 + 3B_2)] - 3\lambda^* B_2/[B_1(B_1 + 3B_2)] \ , \\ B_1 &= 2[\mu^* + (1 - v_f)(\mu^* - \mu)(S_1 - 1)] \ , \\ B_2 &= \lambda^* + (1 - v_f)[2S_2(\mu^* - \mu) + (S_1 - 1)(\lambda^* - \lambda) + 3S_2(\lambda^* - \lambda)] \ . \end{aligned} \tag{A.16}$$

The volume average of the strain field can be written in the form

$$\varepsilon^D_{ij} = \frac{1}{V}\int\limits_D \varepsilon_{ij} dv = \frac{1}{V}\int\limits_D (C^{-1}_{ijkl}\sigma_{kl} + \varepsilon^{**}_{ij}) dv \ . \tag{A.17}$$

Since $\int\limits_D \sigma_{ij} dv = \iint\limits_S \sigma_{ik} x_j n_k ds - \int\limits_D \sigma_{ik,k} x_j dv = 0$, one obtains

$$\varepsilon^D_{ij} = v_f D_{ijkl}\varepsilon^p_{kl} \ , \tag{A.18}$$

where

$$D_{ijkl} = D_1 E^1_{ijkl} + D_2 E^2_{ijkl} \, . \tag{A.19}$$

Acknowledgements

The authors express appreciation to Dr. U. Ramamurty and Dr. H. Fan for helpful discussions on the content of the article. This work of B. Wang was partially supported by the National Science Foundation of China through the Award for Excellent Young Investigators.

References

[1] Gleiter, H.: Nanostructured materials: Basic concept and microstructures. Acta Mater. **48**, 1–29 (2000).

[2] Siegel, R. W., Fougere, G. E.: Mechanical properties of nanophase materials. In: Nanophase materials: synthesis-properties-application (Hadjipanayis, G., Siegel, R. W., eds.), pp. 233–246, 1994.

[3] Kim, H. S., Estrin, Y., Bush, M. B.: Plastic deformation behavior of fine-grained materials. Acta Mater. **48**, 493–504 (2000).

[4] Van Swygenhoven, H., Spaczer, M., Caro, A.: Microscopic description of plasticity in computer generated metallic nanophase samples: A comparison between Cu and Ni. Acta Mater. **47**, 383–398 (1999).

[5] Valiev, R. Z.: Structure and mechanical properties of ultrafine-grained metals. Mat. Sci. Engng **A234–236**, 59–66 (1997).

[6] Wang, N., Wang, Z., Aust, K. T., Erb, U.: Effect of grain size on mechanical properties of nanocrystalline materials. Acta Metall. Mater. **43**, 128–141 (1995).

[7] Carsley, J. E., Milligan, W. W., Hackney, S. S., Aifantis, E. C.: Glasslike behavior in a nanostructured Fe/Cu alloy. Metall. Mater. Trans. A **26A**, 2479–2492 (1995).

[8] Sanders, P. G., Youngdahl, G. J., Weertman, J. R.: The strength of nanocrystalline metals with and without flaws. Mat. Sci. Engng **A234–236**, 77–89 (1997).

[9] Palumbo, G., Thorpe, S. J., Aust, K. T.: On the contribution of triple junctions to the structure and properties of nanocrystalline materials. Scripta Metall. Mater. **24**, 1347–1360 (1990).

[10] Thomas, G. J., Siegel, R. W., Eastman, J. A.: Grain boundaries in nanophase palladium. High resolution electron microscopy and image simulation. Scripta Metall. Mater. **24,** 201–221 (1990).

[11] Mutschele, T., Kirchheim, R.: Hydrogen as a probe for the average thickness of a grain boundary. Scripta Metall. **21**, 1101–1116 (1987).

[12] Kirchheim, R., Mutschele, T., Kieninger, W., Gleiter, H., Birringer, R., Koble, T. D.: Hydrogen in amorphous and nanocrystalline metals. Mat. Sci. Engng **99,** 457–476 (1988).

[13] Palumbo, G., Doyle, D. M., El-Sherik, A. M., Erb, U., Aust, K. T.: Intercrystalline hydrogen transport in nanocrystalline nickel. Scripta Metall. Mater. **27**, 679–696 (1991).

[14] Rice, J. R.: Inelastic constitutive relations for solids: an internal-variable theory and its application to metal plasticity. J. Mech. Phys. Solids **19,** 433–448 (1971).

[15] Zirgler, Z.: Introduction to thermomechanics, 2nd, rev. ed. Amsterdam: North-Holland 1983.

[16] Mura, T.: Micromechanics of defects in solids, 2nd, rev. ed. Martinus Nijhoff 1987.

[17] Mori, T., Tanaka, K.: Average stress in matrix and average energy of materials with misfitting inclusions. Acta Metall. **21**, 373–379 (1973).

[18] Lubliner, J.: Plasticity theory. New York: Macmillan 1990.

[19] Hill, R.: The mathematical theory of plasticity. London: Oxford University Press 1950.

[20] Donovan, P. E.: Yield criterion for $Pd_{40}Ni_{40}P_{20}$ metallic glass. Acta Metall. **37**, 445–462 (1989).

[21] Fan, C., Louzguine, D. V., Li, C., Inoue, A.: Nanocrystalline composites with high strength obtained in Zr-Ti-Ni-Cu-Al bulk amorphous alloys. Appl. Phys. Lett. **75**, 238–249 (1999).

[22] Ramamurty, U., Nagendra, N., Goh T. T., Li, Y.: Effect of crystallinity on the impact toughness of La-based bulk metallic glass. Private communication, 2000.

[23] Shaw, M. C.: In: Mechanical behavior of materials (McClintock, F. A., Argon, A. S., eds.), pp. 443–456. Reading, Mass.: Addison-Wesley 1966.

[24] Tanaka, K., Mori, T.: The hardening of crystals by non-deforming particles and fibers. Acta Metall. **18**, 931–941 (1970).

[25] Fleck, N. A., Hutchinson, J. W.: Strain gradient plasticity. In: Adv. Appl. Mech. **33** (Hutchinson, J. W., Wu, T. Y., eds.), pp. 295–361. New York: Academic Press 1997.

[26] Hutchinson, J. W.: Plasticity at micro scale. Int. J. Solids Struct. **37**, 225–238 (2000).

[27] Gao, H, Huang, Y., Nix, M. D.: Mechanism-based strain gradient plasticity-I. Theor. J. Mech. Phys. Solids **47**, 1239–1263 (1999).

[28] Huang Y., Zhang, L., Guo, T. F., Huang K.-C.: Mixed-mode near-tip fields for cracks in materials with strain-gradient effects. J. Mech. Phys. Solids **45**, 439–465 (1997).

[29] Weng, G. J.: The overall elastoplastic stress-strain relations of dual-phase metals. J. Mech. Phys. Solids **38**, 419–441 (1990).

[30] Sanders, P. G., Eastman, J. A., Weetman, J. R.: Elastic and tensile behavior of nanocrystalline copper and palladium. Acta Mater. **45**, 168–180 (1997).

Authors' addresses: B. Wang, Electro-Optics Technology Center, Harbin Institute of Technology, Harbin 150001, China (E-mail: wangbiao@hope.hit.edu.cn); Z. M. Xiao, School of MPE, Nanyang Technological University, Singapore 639798, Republic of Singapore (E-mail: mzxiao@ntu.edu.sg)